Holographic p-wave Superconductor with Disorder

D. Areán[a], A. Farahi[b], L. A. Pando Zayas[b], I. Salazar Landea[c] and A. Scardicchio[d]

[a] *Max-Planck-Institut für Physik (Werner-Heisenberg-Institut)*
Föhringer Ring 6, D-80805, Munich, Germany

[b] *Michigan Center for Theoretical Physics*
Randall Laboratory of Physics, University of Michigan
Ann Arbor, MI 48109, USA

[c] *Instituto de Física La Plata (IFLP) and Departamento de Física*
Universidad Nacional de La Plata, CC 67
1900 La Plata, Argentina

[c,d] *International Centre for Theoretical Physics (ICTP)*
Strada Costiera 11, I 34014 Trieste, Italy

[d] *Physics Department, Princeton University, Princeton, NJ 08542, USA*

[d] *Physics Department, Columbia University, New York, NY 10027, USA*

[d] *ITS, Graduate Center, City University of New York, New York, NY 10016, USA*

[d] *INFN, Sezione di Trieste, Strada Costiera 11, 34151, Trieste, Italy*

We implement the effects of disorder on a holographic p-wave superconductor by introducing a random chemical potential which defines the local energy of the charge carriers. Since there are various possibilities for the orientation of the vector order parameter, we explore the behavior of the condensate in the parallel and perpendicular directions to the introduced disorder. We clarify the nature of various branches representing competing solutions and construct the disordered phase diagram. We find that moderate disorder enhances superconductivity as determined by the value of the condensate. The disorder we introduce is characterized by its spectral properties and we also study its influence on the spectral properties of the condensate and charge density. We find fairly universal responses of the resulting power spectra characterized by linear functions of the disorder power spectrum.

1   Introduction

The AdS/CFT correspondence [1, 2, 3, 4] provides a window into the dynamics of strongly coupled systems by identifying the underlying field theory with a weakly coupled gravity dual. In recent years the methods and scope of the AdS/CFT have shifted from traditionally QCD-motivated problems to problems in the area of condensed matter systems (see reviews [5, 6, 7, 8], and references therein). In particular, various models of holographic s-wave [9, 10] and p-wave [11, 12] superconductors have been constructed.

Among the various paradigms in condensed matter physics, disorder is a fundamental one as it provides a crucial step away from clean systems toward realistic ones. One striking manifestation of disorder in non-interacting quantum systems is the phenomenon of Anderson localization [13], where the conductivity can be completely suppressed by quantum effects. The study of the interplay between disorder and interactions in quantum systems has seen little progress on the theoretical side. Recently, however, in the context of disordered conductors, Basko, Aleiner and Altshuler presented compelling evidence in favor of a many-body localized phase, based on an analysis of the perturbation theory in electron-electron interaction to all orders [14]. Subsequent works (see [15, 16, 17, 18] and references therein) have confirmed and sharpened the existence of a phase transition separating the weakly and strongly interacting limits of electrons in disordered potentials.

Disorder is also particularly relevant in the context of superconductors; it has a rich history dating back to the pioneering work of Anderson in 1959 [19]. For many years Anderson's theorem, stating that superconductivity is insensitive to perturbations that do not destroy time-reversal invariance (pair breaking), provided the central intuition. Critiques to Anderson's argument were raised, for example, in [20, 21, 22, 23] where the effects of strong localization were considered. More generally, the interplay between interactions and disorder in superconductors cannot be considered settled. In view of this situation, it makes sense to consider alternative models where the problem can be analyzed in full detail.

Indeed, in a previous work [24], we initiated a program of directly studying the role of disorder in holographic superconductors which arguably apply to strongly interacting superconductors. There have been other approaches to disorder in holography [25, 26, 27, 28, 29, 30, 31]. As in [24], we follow a very direct approach to the realization of disorder by coupling an operator to a randomly distributed space-dependent source. Essentially, we directly translate a typical condensed matter protocol into the AdS/CFT framework. Namely, we choose a random space-dependent chemical potential by setting the boundary value of a $U(1)$ electric potential. The main rationale for this choice of disorder relies on

the fact that the chemical potential defines the local energy of a charge carrier placed at a given position x, as it couples to the particle number $n(x)$ locally. Therefore, our choice of disorder replicates a local disorder in the on-site energy. This is the simplest protocol one would implement. Moreover, once disorder is introduced in such an interacting system, all observables will become disordered and, therefore, the physics is not expected to depend on the way disorder is originally implemented.

The direct approach outlined above has now been applied by other authors in the context of holography. For example, it was used to argued for Anderson localization in [32]. Other interesting applications include [33] and [34].

It is worth mentioning that another very important motivation for our work is related to the more general and far-reaching problem of translational invariance in holography. Most holographic models respect translational invariance in the field theory directions. This underlying translational invariance has adverse effects in applications involving transport properties in condensed matter. Since translational invariance implies momentum conservation, it means that the charge carriers have nowhere to dissipate their momentum, resulting in a zero frequency delta function in the optical conductivity which obscures interesting questions such as the temperature dependence of the DC resistivity. A lot of effort has recently been devoted to addressing this shortcoming. Some progress has been reported in [35, 36, 37]. Another approach to momentum dissipation include models of massive gravity [38], [39], [40, 41]. However, this approach struggles with issues of UV completeness of the gravity models used.

The paper is organized as follows. In section 2, we review the construction of the holographic p-wave superconductor. In section 3 we introduce our implementation of disorder and present some typical results. In section 4 we describe the different branches that emerge in our setup and determine which one wins the thermodynamic competition by comparing the free energy. In section 5 we present the disorder phase diagram. Section 6 is devoted to the power spectra of the response. Namely we establish a fairly universal spectral response for the charge density and the condensate as a function of the spectral description of the disordered chemical potential. We conclude in section 7 where we also point out some interesting directions.

2 Review of the holographic p-wave superconductor

To build a holographic p-wave superconductor in 2+1 dimensions we start with the action introduced originally in [11] and further studied in [12]. Namely, we consider the dynamics of a $SU(2)$ Yang-Mills field in a gravitational background:

$$S = \int d^4x \sqrt{-g} \left(\frac{1}{16\pi G_N} (R - \Lambda) - \frac{1}{4q^2} Tr\, F_{\mu\nu}\, F^{\mu\nu} \right).$$
(1)

In the limit where G_N/q^2 is very small, gravity can be considered decoupled and then, the Yang-Mills system is studied on the Schwarzschild-AdS metric:

$$
\begin{aligned}
ds^2 &= \frac{1}{z^2} \left(-f(z)dt^2 + \frac{dz^2}{f(z)} + dx^2 + dy^2 \right), \\
f(z) &= 1 - z^3,
\end{aligned}
$$
(2)

where we have set the radius of AdS, $R = 1$, and the position of the horizon to $z_h = 1$.

In [12] an Ansatz was chosen such that the spatial rotational symmetry is spontaneously broken when the condensate breaking the gauge $U(1)$ symmetry subgroup arises at low temperatures.

The field strength in the action Eq. (1) is given by

$$F^a_{\mu\nu} = \partial_\mu A^a_\nu - \partial_\nu A^a_\mu + f^a_{bc} A^b_\mu A^c_\nu,$$
(3)

and the corresponding Yang-Mills equations of motion:

$$\nabla_\mu F^{a\mu\nu} + f^a_{bc} A^b_\mu F^{c\mu\nu} = 0.$$
(4)

In what follows we specialize to $SU(2)$ with the following generators (further conventions are as in [42]):

$$T_i = \frac{1}{2}\sigma_i, \qquad \{T_i, T_j\} = \frac{1}{2}\delta_{ij}\mathbb{I}.$$
(5)

It is possible to consider more general groups, for example $U(2)$, see [43, 44].

Motivated by condensed matter applications and, in particular superconductivity, we are interested in a system at finite chemical potential which develops an instability at low temperatures. One simple Ansatz that achieves this goal is

$$A = \phi(z)dt\, T_3 + w_x(z)dx\, T_1.$$
(6)

3

Following the AdS/CFT dictionary, one reads field theory information from the boundary data of the gravity fields. Namely, the boundary $(z \to 0)$ values of the fields are:

$$\phi(z) = \mu - \rho\, z + o(z^2)\,,$$
$$w_x(z) = w_x^{(0)} + w_x^{(1)}\, z + o(z^2)\,. \tag{7}$$

The field theory interpretation in terms of these boundary values is as follows: μ is a chemical potential, ρ is the charge density, $w_x^{(0)}$ is the source and $w_x^{(1)}$ is the vacuum expectation value of the vector order parameter. Since we are interested in a spontaneous symmetry breaking we will require the source to vanish $w_x^{(0)} = 0$. Notice that due to the rescaling that allowed us to set the horizon radius $z_h = 1$, the chemical potential μ is actually dimensionless and proportional to the physical chemical potential over the temperature. If one works in the grand canonical ensemble, where the chemical potential is held fixed, the temperature of the system is thus given by $T \propto 1/\mu$. Hence in the rest of the paper we will only talk about μ, in the understanding that it is equivalent to the inverse of the temperature of the boundary field theory at fixed chemical potential.

An intuitive way of understanding the mechanism of condensation is as follows. The gravity mode $w_x(z)$ has an effective mass of the form:

$$m_{eff}^2 = q^2\, g^{tt}\, \phi^2\,. \tag{8}$$

Since $g^{tt} < 0$, as we increase the value of μ the effective mass decreases and goes below the BF bound in a sufficiently large region of space and, consequently, a zero mode of $w_x(z)$ develops at some μ_c. Increasing μ above the critical value, μ_c, leads to the field condensing, and a new branch of solutions with nonzero condensate emerges. This instability is fairly universal, appearing both in the s-wave [9, 10] and p-wave [11, 12] holographic superconductors.

The asymptotic value of μ plays the role of chemical potential in the dual field theory. It is worth mentioning that since the order parameter is determined by the asymptotic value of the field w which is a vector, we have a vectorial order parameter.

To complete the analogy with the superconducting phase transition the conductivities were computed for this system [11, 12], and qualitative agreement was established. More recent studies of this system, some taking into account the gravitational back-reaction, include: [37, 45, 46, 47, 48, 49].

3 Holographic p-wave superconductor with disorder

The main goal in this manuscript is the introduction of disorder in the x-direction of the field theory dual. To be consistent with the equations of motion, we are not allowed to choose the direction of the condensate freely as done in the previous section. We, therefore, consider the following consistent Ansatz for the matter fields:

$$A = \phi(x,z)\, dt\, T_3 + w_x(x,z)\, T_1\, dx + w_y(x,z)\, T_1\, dy + \theta(x,z)\, T_2\, dt \,, \tag{9}$$

where T_i are the $SU(2)$ generators presented before in Eq. (5).

The Yang-Mills equations of motion following from the Lagrangian (1) and the Ansatz (9) are:

$$-\partial_z^2\phi - \frac{1}{f}\,\partial_x^2\phi + \frac{1}{f}(w_x^2 + w_y^2)\phi + \frac{1}{f}\theta\partial_x w_x + \frac{2}{f}w_x\partial_x\theta = 0\,, \tag{10}$$

$$\partial_z^2 w_x + \frac{f'}{f}\partial_z w_x + \frac{1}{f^2}\left(\phi^2 + \theta^2\right)w_x + \frac{1}{f^2}\phi\partial_x\theta - \frac{1}{f^2}\theta\partial_x\phi = 0\,, \tag{11}$$

$$\partial_z^2\theta + \frac{1}{f}\partial_x^2\theta - \frac{1}{f}(w_x^2 + w_y^2)\theta + \frac{1}{f}\phi\partial_x w_x + \frac{2}{f}w_x\partial_x\phi = 0\,, \tag{12}$$

$$\partial_z^2 w_y + \frac{1}{f}\partial_x^2 w_y + \frac{f'}{f}\partial_z w_y + \frac{1}{f^2}\left(\phi^2 + \theta^2\right)w_y = 0\,. \tag{13}$$

These equations of motion satisfy the constraint

$$\phi\partial_z\theta - \theta\partial_z\phi - f\,\partial_z\partial_x w_x = 0\,, \tag{14}$$

which is a consequence of gauge fixing: $A_z = 0$.

As in the previous case, discussed around Eqs. (7), to uncover the physics of the dual field theory we need to examine the boundary values of the supergravity fields. The near boundary asymptotics of the solutions to equations (10-13) is given, at small values of z, by:

$$\phi(x,z) = \mu(x) - \rho(x)\,z + o(z^2)\,, \tag{15}$$

$$w_x(x,z) = w_x^{(0)}(x) + w_x^{(1)}(x)\,z + o(z^2)\,, \tag{16}$$

$$\theta(x,z) = \mu_2(x) - \rho_2(x)\,z + o(z^2)\,, \tag{17}$$

$$w_y(x,z) = w_y^{(0)}(x) + w_y^{(1)}(x)\,z + o(z^2)\,. \tag{18}$$

The values $\mu(x)$ and $\rho(x)$ correspond to space-dependent chemical potential and charge density, respectively. Turning on a chemical potential in the direction T_3 means breaking

$SU(2) \rightarrow U(1)_3$. The functions $w_i^{(0)}(x)$ and $w_i^{(1)}(x)$ are identified, under the holographic duality, with the source and VEV of vectorial operators in the i direction. Finally, $\mu_2(x)$ and $\rho_2(x)$ are, respectively, a new chemical potential and charge density that are sourced by the space-dependent condensate.

The near horizon conditions on the gravity fields are completely determined by regularity of the solution. Regularity, consequently, implies that A_t vanishes at the horizon. Hence, we consider an asymptotic expansion about $z \sim 1$ of the form

$$
\begin{aligned}
\phi(x, z) &= (1 - z)\,\phi_h^{(1)}(x) + (1 - z)^2\,\phi_h^{(2)}(x) + \dots\,, \\
\phi(x, z) &= (1 - z)\,\theta_h^{(1)}(x) + (1 - z)^2\,\theta_h^{(2)}(x) + \dots\,, \\
w_i(x, z) &= w_{ih}^{(0)}(x) + (1 - z)\,w_{ih}^{(1)}(x) + (1 - z)^2\,w_{ih}^{(2)}(x) + \dots\,,
\end{aligned}
\tag{19}
$$

where the ellipses stand for higher order terms.

For numerical reasons, we find it convenient to redefine some of the fields involved in the equations of motion. Namely:

$$
\chi_i(x, z) = (1 - z)\,w_i(x, z)\,.
\tag{20}
$$

In terms of the redefined fields (20) the equations (10-13) take the form

$$
\partial_z^2 \phi + \frac{1}{f}\,\partial_x^2 \phi - \frac{\chi^2}{(1 - z)^2 f}\phi - \frac{1}{(1 - z)\,f}\,(2\chi_x\,\partial_x\theta + (\partial_x\chi_x)\,\theta) = 0\,,
\tag{21}
$$

$$
\partial_z^2 \theta + \frac{1}{f}\partial_x^2 \theta - \frac{\chi^2}{f(1 - z)^2}\theta + \frac{2\chi_x\,\partial_x\phi + (\partial_x\chi_x)\,\phi}{f(1 - z)} = 0\,,
\tag{22}
$$

$$
\partial_z^2 \chi_x + \left(\frac{f'}{f} + \frac{2}{1 - z}\right)\partial_z\chi_x + \frac{2f^2 + (1 - z)\,f\,f' + (1 - z)^2(\theta^2 + \phi^2)}{(1 - z)^2\,f^2}\chi_x +
$$
$$
+\frac{1 - z}{f^2}\,(\phi\,\partial_x\theta - (\partial_x\phi)\,\theta) = 0\,,
\tag{23}
$$

$$
\partial_z^2 \chi_y + \frac{1}{f}\partial_x^2 \chi_y + \left(\frac{f'}{f} + \frac{2}{1 - z}\right)\partial_z\chi_y + \left[\frac{2}{(1 - z)^2} + \frac{1}{f^2}(\theta^2 + \phi^2) + \frac{f'}{f\,(1 - z)}\right]\chi_y = 0\,,
\tag{24}
$$

where $\chi^2 = \chi_x^2 + \chi_y^2$.

This redefinition leads to a simpler set of boundary conditions:

$$
\begin{aligned}
\chi_i(x,0) &= 0, & \theta(x,0) &= 0, & \phi(x,0) &= \mu(x), \ \text{UV} \ z \to 0, \\
\chi_i(x,1) &= 0, & \theta(x,1) &= 0, & \phi(x,1) &= 0, & \text{IR} \ z \to 1.
\end{aligned}
\tag{25}
$$

This choice of boundary conditions corresponds to a spontaneous breaking of the $U(1)$ symmetry with order parameter $\langle \mathcal{O} \rangle \propto w_i^{(1)}(x)$. From now on we use the angle brackets associated with $\mathcal{O}$ exclusively to refer to the average over x. Moreover, we choose the condition $\mu_2 = 0$ (vanishing source for the charge density in the T_2 direction) since we want a disordered version of the p-wave superconductor. Hence, the charge density ρ_2 will be spontaneously induced. In this case, since the symmetry of our action (1) is the whole $SU(2)$, we are effectively realizing a two-component superfluid as recently discussed in the holographic framework in [42] following original ideas of [50], an important phenomenological paradigm in various condensed matter situations. We will however not pursue these questions in the present manuscript.

It is worth noticing that there are two simplified situations that might be taken into account, given that they might include all the interesting physics but require less computing power. It is easy to see that the equations (10-13) allow to consistently set $w_x = \theta = 0$ or $w_y = 0$. This is equivalent to going to the two limits in which the system condenses in the direction of the noise or in the direction perpendicular to the noise. We will devote ample attention to these branches in section 4.

3.1 Introducing disorder

We are interested in solving the system given by equations (10 - 13) in the presence of disorder. Let us take the following form for the noisy chemical potential:

$$
\begin{aligned}
\mu(x) &= \mu_0 + \epsilon \sum_{k=k_0}^{k_*} \sqrt{S_k} \cos(k\, x + \delta_k) \\
&= \mu_0 + \epsilon \sum_{k=k_0}^{k_*} \frac{1}{k^\alpha} \cos(k\, x + \delta_k),
\end{aligned}
\tag{26}
$$

where δ_k is a random phase for each k and S_k is the power spectrum. In the limit of a large number of modes the form of Eq. (26) tends to a Gaussian distributed random function, the power of $1/k$ determines the differentiability properties of $\mu(x)$.

This means that our noise will be continuous but without well defined derivatives. We discretize the space, and impose periodic boundary conditions in the x direction, leading to k with values:

$$k_n = \frac{2\pi \, n}{L} \quad \text{with} \quad 1 \leq n \leq \frac{L}{2a_x}, \tag{27}$$

where L is the length in the x direction of our cylindrical space, and a_x is the lattice spacing in x. Note that there is an IR scale given by k_0 and a UV scale defined by k_*. Notice that the UV scale k_* is given by π/a_x, and was chosen to saturate the Nyquist limit[1]. In some cases to attain a higher numerical accuracy we would limit our numerical calculations to a smaller number of modes, k_j, selected from the general set, k_n, in (27).

For the realization of the noise following Eq. (26) we characterize the strength of disorder by introducing w as $\epsilon = \frac{2}{5}\mu_0(w/10)$, where $w = 0$ corresponds to the homogeneous case and $w \sim 12$ is the largest $\epsilon_{max} \sim \frac{12}{25}\mu_0$. We choose this maximum value of the strength by demanding that $\mu(x)$ remains positive. Notice that this maximum value depends also on the length of the system L and the power α characterizing the power spectrum . The values mentioned before correspond to $L = 2\pi$ and $\alpha = 1.50$, which were the most broadly used throughout the paper. This is a somewhat heuristic choice, but we have then confirmed numerically that indeed $\mu(x) > 0$ for all the choices of (μ_0, ϵ).

Our definition of w corresponds, in the standard solid state notation, to $1/k_F \, l$, where k_F is the Fermi momentum and l is the mean free path [51]. With this choice of scales we have essentially two dimensionless quantities T/μ_0 and the strength of the noise w.

Numerical Methods

In order to solve the system of PDEs we have discretized it on a rectangular lattice of size $N_z \times N_x$, where N_z and N_x correspond, respectively, to the number of points in the z and x directions. For most of the simulations we used planar lattices for the x direction, and Chebyshev grids along z. Consequently, the discretization of the derivatives was performed using pseudo spectral methods (with periodic boundary conditions in the x direction). To find solutions we employed a Newton-Raphson algorithm on lattices with a typical size of 25×50.

Finally, we cross-checked our solutions by solving the system through a relaxation method. In this case we used planar grids for both x and z directions, and a finite difference scheme

---

[1]Nyquist frequency is the highest frequency that can be reconstructed from a signal given a sample rate. In order to recover all Fourier components of a periodic waveform, it is necessary to use a sampling rate at least twice the highest waveform frequency. This can be understood from the fact that there are two Fourier coefficients to fit for each frequency.

for the derivatives. The solutions were found via a relaxation method on lattices with a typical size of 150×150.

In Figs. 1, 2 we plot the results of a single simulation. In Fig. 1 we present the random chemical potential $\mu(x)$ (upper left panel) together with the solutions for the fields ϕ, θ, χ_x resulting from solving the system (21-24) with that chemical potential as boundary condition. Instead, in Fig. 2 we present the boundary data read from this same solution. This introduction of disorder then leads to the appearance of a charge density and condensate in some cases which we plot in those figures. In a sense one could view the gravity equations of motion as a tool that provides precise answers to the question: Given a random chemical potential in a strongly coupled system with a superconducting transition, what is the value of the condensate and the charge density that the system uses to respond to the random chemical potential?
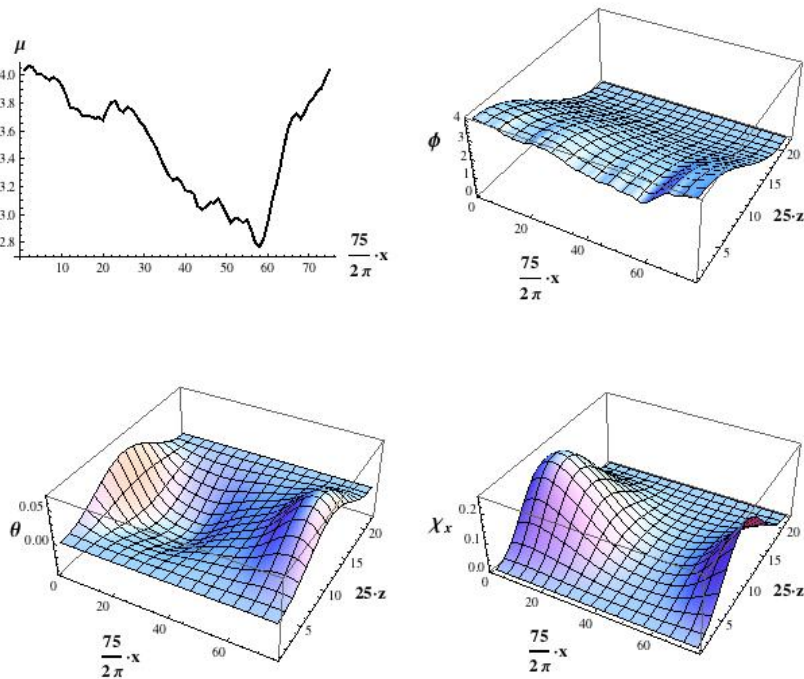

Figure 1: Example of a simulation corresponding to a noisy chemical potential with $w = 3.50$, $\alpha = 1.50$, and $\mu_0 = 3.50$ below the critical value of the homogeneous chemical potential ($\mu_c = 3.66$). We plot the original spatial-dependent chemical potential on the upper-left panel and the corresponding solutions for the fields ϕ, θ and χ_x ($\chi_y = 0$ for this solution) on the other three panels.

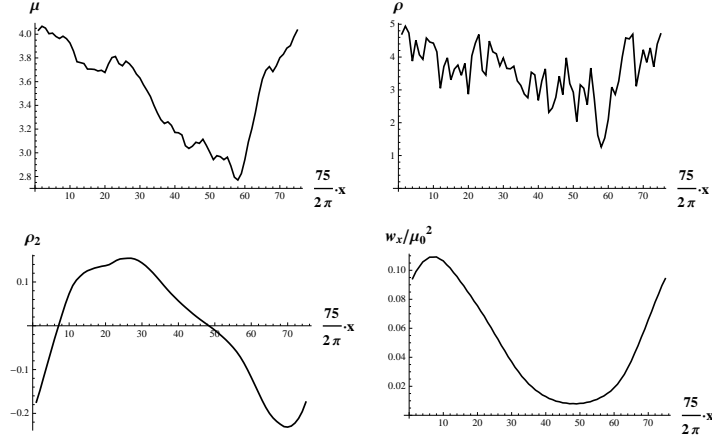Notice that the response to the source $\mu(x)$ is noisier for the VEV corresponding to the

Figure 2: Boundary data corresponding to the same simulation as in Fig. 1. From the upper left panel and in clockwise sense: $\mu(x)$, $\rho(x)$, $\omega_x(x)$, and $\rho_2(x)$.

same field, that is, $\rho(x)$; while the VEVs realized by other fields, that is $w_x(x)$ and $\rho_2(x)$, are visibly smoother. We will investigate this behavior in more detail in section 6.

It is worth pointing out, and we will use this result in the upcoming sections, that we find that for a chemical potential below the critical (in the homogeneous case), there are values of the strength of the disorder that render the expectation value everywhere non-vanishing; this is our definition of arriving at the superconducting phase via disorder.

3.2 Thermodynamic limit and self-averaging condensate

In the context of condensed matter physics it is quite important to consider the thermodynamic limit. Namely, to study the properties of the system in the limit where its size goes to infinity. The thermodynamic limit plays a particularly important role in systems dominated by quenched randomness. In this subsection we address some issues related to the thermodynamic limit as they apply to the the problem at hand.

Let us review, once more, all the scales involved in the problem, both, physical and numerical. The three physical dimensionless scales of the problem are T/μ, w, and $L\mu$ corresponding respectively to the temperature, the strength of the noise, and the length of the system in the x direction, all measured relative to the chemical potential. Since we are solving the problem numerically using a lattice we have two extra scales: a_x and a_z which are the sizes of cells along the x and the z directions.

Discussing the thermodynamic limit is more than a mere academic question. Given that the realization of disorder is intrinsically related to our way of solving the system we need
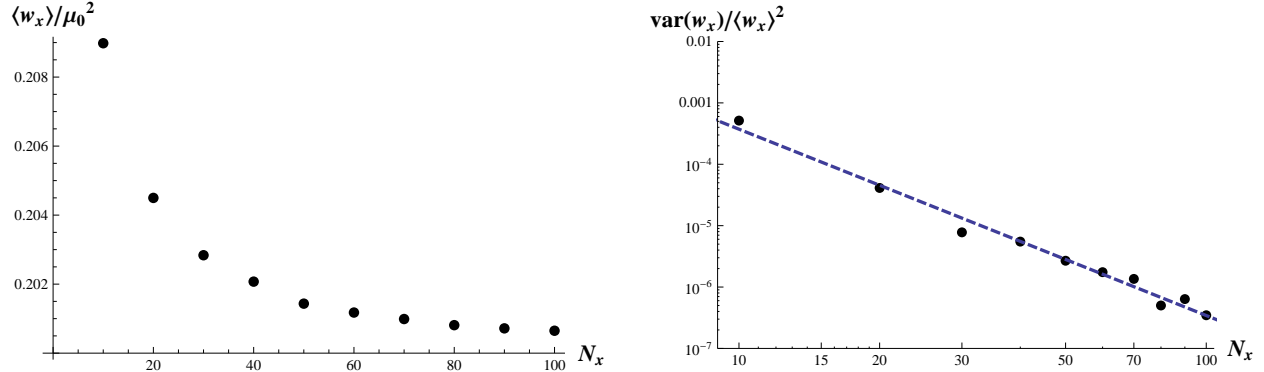
10

Figure 3: On the left panel we plot the average of the condensate versus the number of lattice sites N_x, notice that it stabilizes in the thermodynamic limit. The right panel shows the variance of the condensate versus N_x, and the blue dashed line shows the fit $\log(\mathrm{var}(w_x)/\langle w_x \rangle^2) = -0.90 - 3.03 \log(N_x)$. These figures show that the condensate w_x is self-averaging. The data results from averaging over 50 realizations of a noisy chemical potential with $\alpha = 0$, $\mu_0 = 4.20$, and w such that $w^2 = 160/N_x$ (so that the variance of the noisy chemical potential is kept constant as N_x is increased).

to show that there is a limit to which we are truly approximating. In general, we expect that in the thermodynamic limit certain quantities will be self-averaging. A property X is self-averaging if most realizations of the randomness have the same value of X. More precisely, in the numerical context we use that: The system is said to be self-averaging with respect to property X if

$$\frac{< X_n^2 > - < X_n >^2}{< X_n >^2} \to 0, \tag{28}$$

as the size, n, of the system goes to infinity. Here the angular brackets denote averages over the realizations of the quenched randomness of the system and X_n is the value of property X when the system has size n [52, 53].

We will define our thermodynamic limit as the limit in which the correlation length of the disorder is negligible with respect to the length of the system. In order to do so we will work with flat spectrum noise, which corresponds to setting $\alpha = 0$ in Eq. (26). Then the scale a_x (wich sets $k_* = \pi/a_x$) will determine the correlation length of the disorder in our lattice[2]. Increasing the number of points N_x of the lattice in the x direction while keeping the length of the system fixed will now imply to decrease the correlation length of the noise with respect to the size of the system. Using this prescription, we now study the

---

[2]Even though setting $\alpha = 0$ would correspond to uncorrelated noise, working on a lattice introduces a numerical correlation length since the solutions are blind to wavelengths shorter than the lattice spacing.
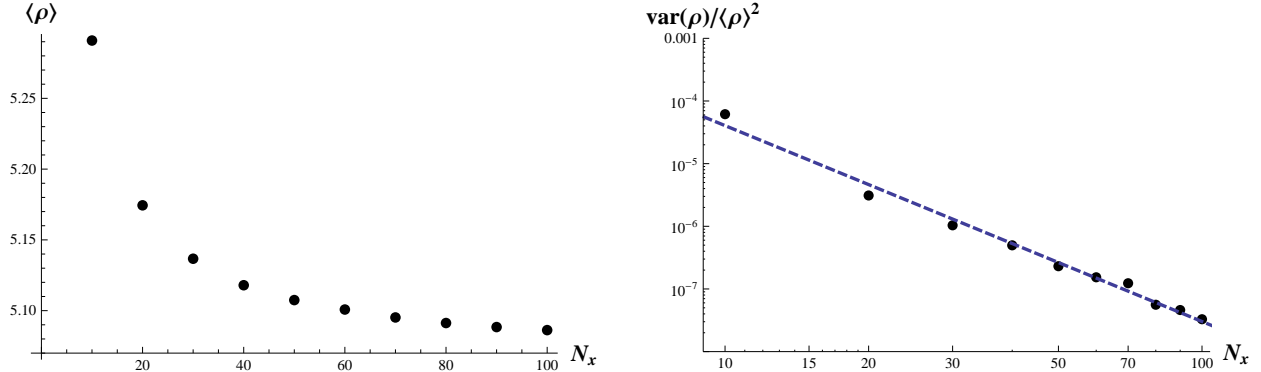
Figure 4: On the left we show the average of the charge density ρ versus the number of lattice sites N_x, while on the right we plot the variance of ρ versus N_x. The blue dashed line results from the fit $\log(\mathrm{var}(\rho)/\langle\rho\rangle^2) = -2.92 - 3.13 \log(N_x)$. These plots follow from the same set of data as those in Fig. 3.

self-averaging property of the condensate in the x-direction, w_x. We claim that the average of the condensate stabilizes, while its variance goes to zero. Moreover, we provide numerical evidence that this vanishing goes as a power law $\sim N_x^{-3}$ (see Log-Log plot in Fig. 3).

The same procedure as described above can be applied to study the self-averaging property of the charge density, ρ. The result is presented in figure 4, which clearly shows that the charge density is indeed self-averaging in the thermodynamic limit.

Finally, as in the previous section, in Figs. 5, 6, we now present a simulation; but this time for the case of uncorrelated noise (Eq. (26) with $\alpha = 0$). The average value of the chemical potential $\mu_0 = 3.5$ is again below the critical for the homogeneous case $\mu_c = 3.66$. Yet again, as can be seen in Fig. 6, by turning on a strong enough noise ($w = 3.5$) we arrive at a nowhere vanishing condensate, indicating a transition to the superconducting phase.

4 Free energy and competing solutions

As already anticipated when we wrote the system of equations in section 3, there are different branches or consistent truncations of the system of equations (21-24). One could expect three main types of solutions:

- Solutions with $\chi_x \equiv 0$ and also $\theta \equiv 0$, we will denote these solutions by Y, since the vector order parameter lies in the direction transverse to the noise. Note that in this approximation the system (21 - 24) reduces significantly. In particular, equations (22)
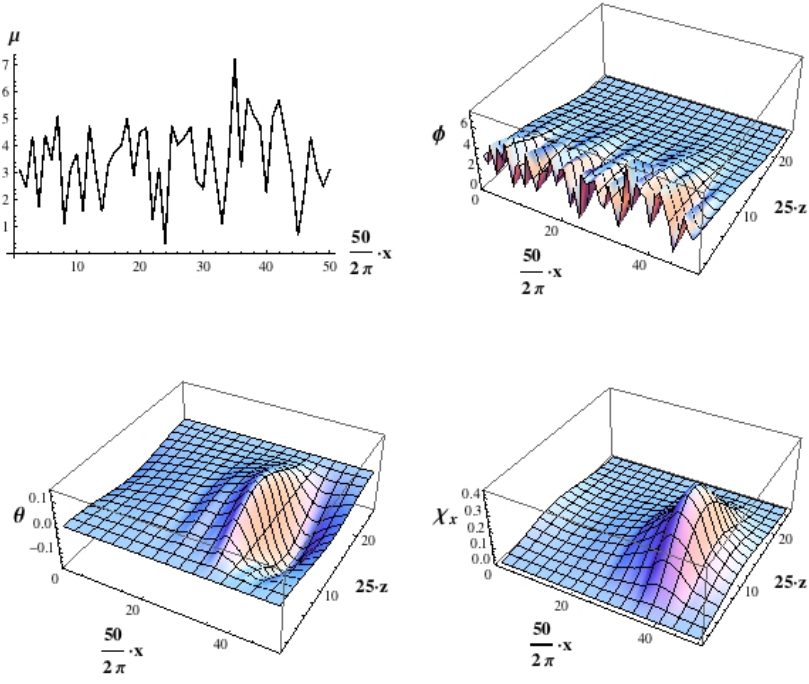
Figure 5: Example of a simulation corresponding to a noisy chemical potential with $\alpha = 0$, $w = 3.50$, and $\mu_0 = 3.50$ below the critical value of the homogeneous chemical potential ($\mu_c = 3.66$). We plot the original spatial-dependent chemical potential on the upper-left panel, and the corresponding solutions for the fields ϕ, θ and χ_x ($\chi_y = 0$ for this solution) on the other three panels.
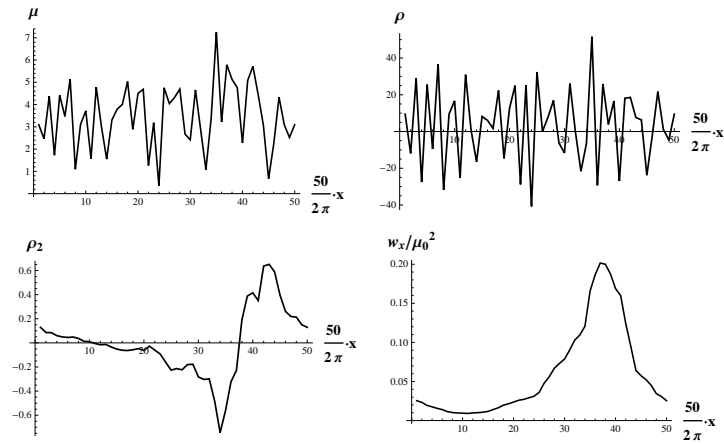

Figure 6: Boundary data corresponding to the same simulation as in Fig. 5. From the upper left panel and in clockwise sense: $\mu(x)$, $\rho(x)$, $\omega_x(x)$, and $\rho_2(x)$.

and (23) are identically satisfied.

- Solutions where $\chi_y \equiv 0$, we denote them by X, as they correspond to a vector condensate along the x direction. In this limit the system of equations (21 - 24) leads to a system with equation (24) trivially satisfied.

- A third possibility would be that of solutions where all functions in the system (21 - 24) are nonzero. These would correspond to a vector condensate pointing along an intermediate direction in the xy plane. However, our numerics indicate that these solutions do not exist.

Let us elaborate a bit more about the absence of solutions where the condensate lies along an intermediate direction in the xy plane. As is clear from the equations, in the absence of noise the system in the normal phase is rotational invariant. Therefore, symmetry-breaking solutions with the condensate along any arbitrary direction on the plane are equivalent. However, as soon as some noise is turned on, our numerics converge to solutions with the condensate being either parallel or orthogonal to the noise. We checked this fact by starting from a broad family of seeds.

We will now study the free energy of the X and Y solutions to decide which of them is energetically favorable. The free energy of the system is given in terms of the on-shell action (1) as

$$
\begin{aligned}
\Omega &= -\frac{T S_{\text{on-shell}}}{L_y L} = \\
&= -\frac{1}{4L} \int_0^L dx\, \mu\, \rho + \frac{1}{4L} \int_0^L dx \int_0^1 dz\, \frac{1}{f} \left[(\theta^2 + \phi^2)(w_x^2 + w_y^2) + w_x(\phi\, \partial_x \theta - \theta\, \partial_x \phi) \right] \,,
\end{aligned}
\tag{29}
$$

where L_y is the length of the system in the y direction; this is a regulator we need in order to get a finite result and will simply cancel out when integrating along the y direction since the solutions are y independent.

In Fig. 7, we plot the free energy for the two kinds of superconducting solutions, together with that of the normal phase[3]. We observe that when it exists the X solution has always lower free energy. Therefore, in the rest of the paper when we refer to the superconducting phase we will restrict ourselves to the X solutions, namely those with condensate pointing in the direction parallel to the noise.

---

[3]In the normal phase $\theta = \chi_x = \chi_y = 0$, and the system (21-24) reduces to the equation (21). The normal phase solution exists for all values of μ.
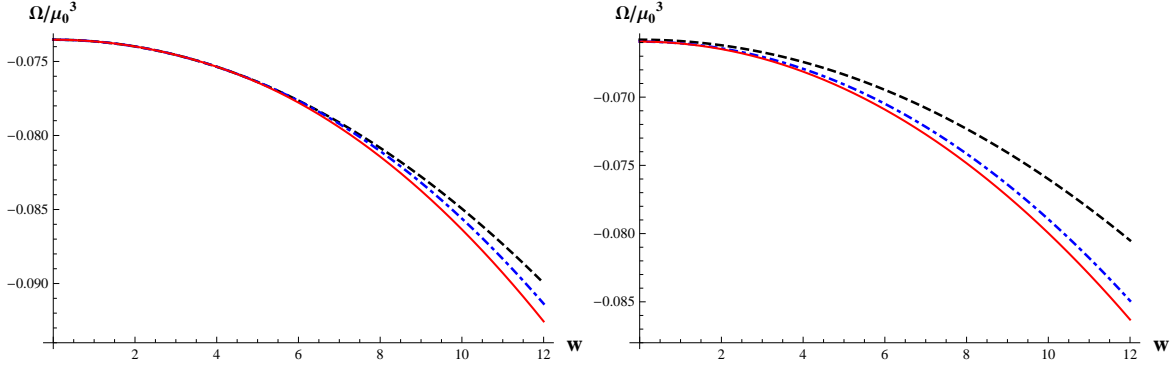
Figure 7: Free energy of competing solutions as a function of the strength of the disorder, w. We consider values of μ_0 below and above the critical one. The left panel corresponds to $\mu_0 = 3.4 < \mu_c$, and the right one to $\mu_0 = 3.8 > \mu_c$ (both with $\alpha = 1.50$). The black dashed line corresponds to the normal phase solution, the blue dot-dashed line to the Y solution, and the red solid line to the X solution. These plots result from averaging over 5 realizations on lattices of size 22×40.

Another observation following from Fig. 7 is that for the panel corresponding to $\mu_0 = 3.4 < \mu_c$, all solutions coincide up to a noise strength $w \sim 6$. This reflects the fact that for $w < 6$ only the solution corresponding to the normal phase exists.

We shall now provide a heuristic explanation for the fact that the X solution is energetically favorable (see [54, 55] for similar arguments). The key observation follows from comparing the equations for the fields w_x and w_y, namely Eqs. (11-13), which we reproduce for convenience

$$\partial_z^2 w_x + \frac{f'}{f}\partial_z w_x + \frac{1}{f^2}\left(\phi^2 + \theta^2\right)w_x + \frac{1}{f^2}\phi\partial_x\theta - \frac{1}{f^2}\theta\partial_x\phi = 0\,, \tag{30}$$

$$\partial_z^2 w_y + \frac{f'}{f}\partial_z w_y + \frac{1}{f^2}\left(\phi^2 + \theta^2\right)w_y + \frac{1}{f}\partial_x^2 w_y = 0\,, \tag{31}$$

We can, for example, consider that the mode w_y is governed by an effective mass of the form:

$$m_{w_y}^2 \propto -\frac{1}{f^2}\left(\phi^2 + \theta^2\right) - \frac{1}{w_y f}\partial_x^2 w_y. \tag{32}$$

As noticed already in [55] the last term contributes a positive amount to the effective mass and impedes condensation[4]. Note, however, that the situation is different for the equation

---

[4]Notice that at linear level one could Fourier transform the equation and consider the effect of a single wave by replacing ∂_x by $i\,k$.

describing the effective mass for the mode w_x.

$$m^2_{w_x} \propto -\frac{1}{f^2}\left(\phi^2 + \theta^2\right) - \frac{1}{w_x f^2}\left(\phi\partial_x\theta - \theta\partial_x\phi\right) . \tag{33}$$

There is no term $\sim \partial^2_x w_x$ impeding condensation, and it can be argued that the last term in the above effective mass is small, since the derivatives cancel at linear level. Thus, condensation of the mode w_y seems to be disfavored while for the mode w_x it is not. Then, one may expect the free energy of the X solution to be lower than that of the Y solution, as our numerics show.

Finally, let us speculate on the consequences the outcome of this free energy computation may have for more realistic systems with bidimensional inhomogeneities. Since it turns out that the solutions with condensate parallel to the noise are always thermodynamically preferred, one would expect that in the presence of disorder in two spatial directions the condensate would point in the stiffest direction, thus following the gradient of the bidimensional noise.

5 Toward the disordered phase diagram

In this section we present the phase diagram of the disordered holographic p-wave superconductor. The key strategy is to repeat the simulations outlined in section 3 with a random chemical potential $\mu(x)$ given by Eq. (26), enough times so that we develop meaningful statistics.

One of our main results is the dependence of the condensate on the strength of the disorder, w, presented in Fig. 8. The results are qualitatively similar to the s-wave results [24]. There are, however, some differences. First, the saturation for large values of μ_0 is different as it seems that the condensate takes relatively larger values of the average chemical potential with respect to the critical one to stabilize. This observation is somewhat marred by the fact that, in general, going to very high values of the chemical potential leads to a region where back-reaction has to be included and, therefore, renders the result in the probe limit unreliable. Second, there seems to be the case that larger values of the chemical potential for the p-wave superconductor allow for an enhancement of the condensate with a higher slope that larger values for the s-wave. There are, certainly, some similarities. For example, as in [24], the curves are noisier at large disorder strength and even noisier for lower values of the chemical potential. It could be suspected that such behavior is the result of numerical limitations but we have run extensive simulations to that effect and verified

that the effect is real and has to do more with the nature of the system of equations in this regime of parameters.
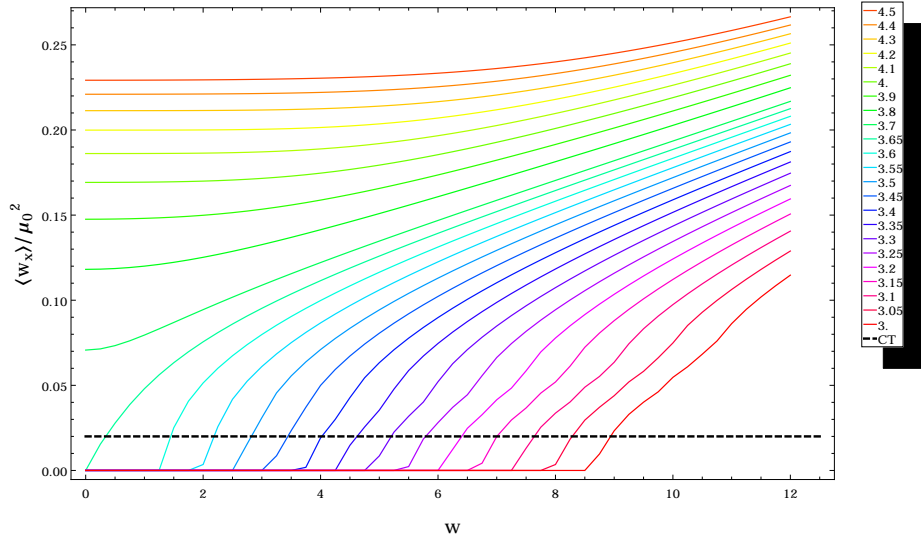

Figure 8: Spatial average of the condensate as a function of the strength of disorder. Each line corresponds to an average over 10 realizations of noise (with $\alpha = 1.50$) on a lattice of size 22×40. The value of the condensate grows with increasing disorder strength, w. Each line corresponds to a value of μ_0 as indicated on the legend, but for the black dashed line which, as explained in the text, marks the cut off used to define the critical temperature.

To make direct contact with the condensed matter literature we propose a disordered phase diagram in Fig. 9 where we track the value of the critical temperature of the normal to superconductor phase transition as a function of the strength of the disorder. Let us explain, for the benefit of clarity how we have proceeded. Since the value of the condensate increases with the the strength of the disorder, we have determined a value of the condensate above which we consider the system in the superconducting phase (black dashed line in Fig. 8). We then read the average chemical potential and use the fact that the only relevant scale is μ/T to determine the critical temperature. Let us advance a potential criticism to out method. Clearly, it would have been more relevant to compute the conductivities and determine the phase diagram based on a conductivity criterion [56]; we expect, as in all previous cases, that there is a direct relation between the existence of a condensate and the transport properties of the holographic solutions. One important aspect of Fig. 8 is its robustness. Namely, the precise form of the phase diagram varies quantitatively depending on where precisely we draw the cut off line defining the "appearance" of a nonzero condensate. However, qualitatively it is clear from the plot that the conclusions are stable with respect

to parallel shifts of the position of this cut off line.

Finally, let us try and explain the mechanism behind this enhancement of the critical temperature. Looking at Eq. (33) it is not evident that the noise would enhance condensation by lowering the effective mass. Actually the effect of the noise on the average (along x) of that effective mass is almost negligible. However, the noise does have the effect of producing regions (in the x direction) where the effective mass is below the critical value for condensation. When these regions are large enough they trigger the condensation, resulting in solutions where the condensate is nonzero along the whole sample (see Figs. 2, 6); even in the regions where the chemical potential is below its critical value (for the homogeneous case) the condensate is nonzero.
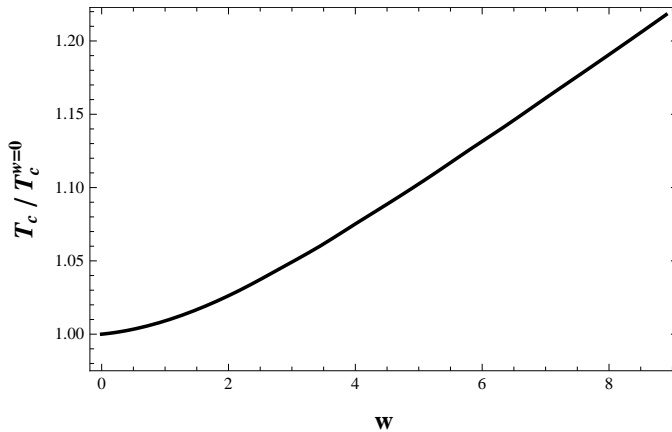

Figure 9:   Enhancement of T_c with the noise strength w ($T_c^{w=0}$ stands for the critical temperature in the absence of disorder).

6   Spectral properties and disorder

In previous sections we have mostly focused on the average properties of the condensate and the charge density. For example, in Fig. 8 we followed the average value of the condensate as a function of the strength of the noise. Although this averaging is a good proxy at first, it is instrumental to the nature of disorder that we look into properties depending on the spatial coordinate x. In this section we will go beyond that first order averaging study. Following [24] we continue the study of the spectral properties of some of the quantities characterizing our system. Our goal is to gain a quantitative understanding.

As in [24], we establish certain universality of the power spectra of the condensate and charge density as functions of the power spectrum of the signal defining the noise. Namely,

for a given random signal with power spectrum of the form $k^{-2\alpha}$ we study the power spectrum of the condensate $k^{-2\Delta(\alpha)}$, of the charge density $k^{-2\Gamma(\alpha)}$, and of the ρ_2 charge density $k^{-2\Gamma_2(\alpha)}$; and report some interesting universal behavior. We interpret this behavior as a particular form of renormalization of small wave-lengths. We argue that this kind of smoothing/roughening points to a renormalization of sorts, where higher harmonics in $\mathcal{O}$ are suppressed or enhanced with respect to their spectral weight in μ.
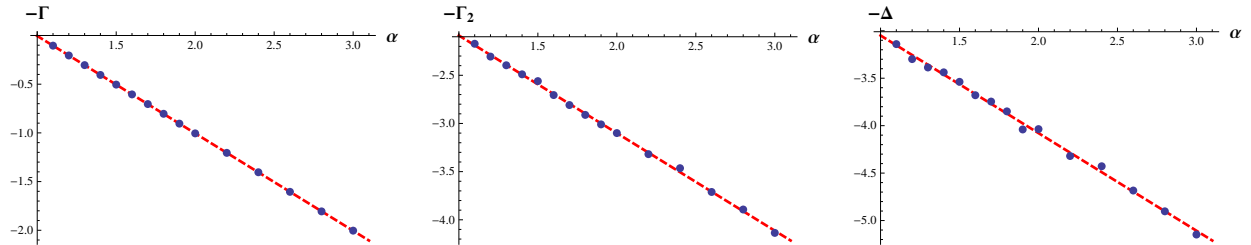

Figure 10: Renormalization of the disorder: Charge density ρ: $\Gamma = -1.00 + 1.00\,\alpha$ (left panel), charge density ρ_2: $\Gamma_2 = 1.07 + 1.01\,\alpha$ (middle panel), and condensate: $\Delta = 2.02 + 1.03\,\alpha$ (right panel). This plot was made considering $L = 2\pi$, $\mu_0 = 4$, $w = 1$, and averaging over 5 realizations on a lattice of size 22×75.

Let us now carefully describe our setup. To characterize this renormalization quantitatively we take a boundary chemical potential of the form presented in equation (26), but now considering different values for α (the choice of α determines the degree of differentiability -smoothness- of the initial profile). To make the concept of renormalization more precise we will study the power spectrum of the modes characterizing the response of our system (the condensate, charge density ρ, and charge density ρ_2), as a function of the input power spectrum determining our noise. This input power spectrum of $\mu(x)$ is essentially proportional to $k^{-2\alpha}$. Remarkably, the power spectrum of the condensate $\mathcal{O}(x)$ is numerically well approximated by $k^{-2\Delta}$ (see the rightmost panel of Fig. 10). We find $\Delta \simeq 2.02 + 1.03\alpha$, which is clearly larger than α, meaning that the weight of the high-k harmonics is smaller in $\mathcal{O}$ than in μ. The power spectrum of the charge density ρ is very well approximated by $k^{-2\Gamma(\alpha)}$ (Fig. 10 left panel) with $\Gamma \simeq -1.00 + 1.00\alpha$, which implies that for the charge density the weight of the high-k harmonics is larger than in the spectrum of μ. As for the charge density ρ_2, again the spectrum approximates very well to a power law $k^{-2\Gamma_2(\alpha)}$ (Fig. 10 middle panel), with $\Gamma_2 \simeq 2.02 + 1.03\alpha$. As for the condensate the weight of the high-k harmonics is smaller than in μ.

Let us stress that the spectra of all the response functions are given by power laws, and moreover, the exponent of these response power laws is always of the form $\sim \alpha + \text{integer}$.

This universality of RG is one of the main observations of our work and its origin seems to be in the strongly coupled nature of the problem. The weak field theory intuition would dictate that Δ should be well approximated by the conformal dimension associated with the order parameter and here we verify that it is not.

It is also interesting to point out that this behavior does not depend on any of the parameters of our theory, i.e. L, T/μ or w. This means that we can redo Fig. 10 for the charge density in the normal phase. This particular case is interesting, since the theory becomes linear and we can therefore separate variables. Being that the case, we can recompute the power spectrum solving the equations of motion using a simple $Mathematica$'s NDSolve command. In this case we get $\Gamma = -1.00 + 1.00\,\alpha$, which agrees with the result presented in Fig. 10. It is worth mentioning that the same scalings were found in [24] for the s-wave holographic superconductor, and similar ones have been observed in a related holographic model by other authors in [33].

7   Conclusions

In this paper we have studied the influence of disorder in the holographic p-wave superconductor. We have found that moderate disorder enhances the value of the order parameter and accordingly of the critical temperature. We have also discussed various branches of solutions that appear in this particular setup since different solutions are characterized by the dominant direction of the condensate.

We have established that the dominant solution, according to its free energy, is the one with the condensate along the x-direction. We have also established that the condensate, $\langle\mathcal{O}_x\rangle/\mu^2$, is enhanced with the disorder. Moreover, we have demonstrated the self-averaging property of $\langle\mathcal{O}_x\rangle$ under Gaussian and uncorrelated randomness. We identify this enhancement with the ulterior enhancement of superconductivity. The phase diagram is similar to the s-wave superconductor reported in [24] and we presented its quantitative form in section 5. The key property is that the curve delimiting the normal and superconducting phase shows an enhancement of the superconductivity with mild disorder. We have also studied some universal properties of the power spectrum of the corresponding condensate and charge density. We have found that the response is largely governed by a simple linear relation depending on the power spectrum of the random chemical potential. These results expand those presented first in [24] to the case of a disordered holographic p-wave superconductor. Similar behavior was also reported in [33] in the perturbative regime for a neutral scalar,

and by some of the authors in gravity duals of brane intersections [56]. One of our main results, the enhancement of superfluidity with mild disorder, is aligned with experimental and numerical claims of p-wave superfluidity enhancement by disorder [57, 58].

We would like to finish by highlighting a few problems that are particularly interesting to us and some of which we hope to pursue in future works. Having constructed the disordered solutions in [24] and the present manuscript, it is natural to study transport properties and, in particular, the conductivities. It would also be interesting to understand the effects of disorder in more general types of holographic p-wave superconductors. Recall that this type of superconductors present a particularly interesting challenge to Anderson's theorem given its directional order parameter. Some interesting models include [12] and its extension to $p_x + i p_y$ along the lines of [59]. A recent study of conductivity in p-wave superconductors was presented in [37], where some phenomenological similarities with high temperature cuprate superconductors were found even in a translational invariant holographic model. It would be interesting to study the persistence or modification of such properties under the effect of introducing disorder as a way of breaking translational invariance in these and similar systems.

Finally, as in [24], we have established the existence of fairly universal response of the condensate and the charge density to the power spectrum of the random disorder. We view this as evidence of some universality in cases of strongly coupled systems under a sort of disorder renormalization. On the other hand, for very small values of k_0, we found evidence of a new scaling for the expectation values of one point functions. We expect to study this potential universality in more detail in the future [56].

Acknowledgments

References

[1] J. M. Maldacena, *The large N limit of superconformal field theories and supergravity*, *Adv. Theor. Math. Phys.* **2** (1998) 231–252, [hep-th/9711200].

[2] E. Witten, *Anti-de Sitter space and holography*, *Adv. Theor. Math. Phys.* **2** (1998) 253–291, [hep-th/9802150].

[3] S. Gubser, I. R. Klebanov, and A. M. Polyakov, *Gauge theory correlators from noncritical string theory*, *Phys.Lett.* **B428** (1998) 105–114, [hep-th/9802109].

[4] O. Aharony, S. S. Gubser, J. M. Maldacena, H. Ooguri, and Y. Oz, *Large N field theories, string theory and gravity*, *Phys. Rept.* **323** (2000) 183–386, [hep-th/9905111].

[5] S. A. Hartnoll, *Lectures on holographic methods for condensed matter physics*, *Class.Quant.Grav.* **26** (2009) 224002, [arXiv:0903.3246].

[6] C. P. Herzog, *Lectures on Holographic Superfluidity and Superconductivity*, *J.Phys.* **A42** (2009) 343001, [arXiv:0904.1975].

[7] J. McGreevy, *Holographic duality with a view toward many-body physics*, *Adv.High Energy Phys.* **2010** (2010) 723105, [arXiv:0909.0518].

[8] S. Sachdev, *Condensed Matter and AdS/CFT*, *Lect.Notes Phys.* **828** (2011) 273–311, [arXiv:1002.2947].

[9] S. A. Hartnoll, C. P. Herzog, and G. T. Horowitz, *Building a Holographic Superconductor*, *Phys.Rev.Lett.* **101** (2008) 031601, [arXiv:0803.3295].

[10] S. A. Hartnoll, C. P. Herzog, and G. T. Horowitz, *Holographic Superconductors*, *JHEP* **0812** (2008) 015, [arXiv:0810.1563].

[11] S. S. Gubser, *Colorful horizons with charge in anti-de Sitter space*, *Phys.Rev.Lett.* **101** (2008) 191601, [arXiv:0803.3483].

[12] S. S. Gubser and S. S. Pufu, *The Gravity dual of a p-wave superconductor*, *JHEP* **0811** (2008) 033, [arXiv:0805.2960].

[13] P. Anderson, *Absence of Diffusion in Certain Random Lattices*, *Phys.Rev.* **109** (1958) 1492–1505.

[14] D. Basko, I. Aleiner, and B. Altshuler, *Metal-insulator transition in a weakly interacting many-electron system with localized single-particle states*, Annals of Physics **321** (2006), no. 5 1126 – 1205.

[15] V. Oganesyan and D. A. Huse, *Localization of interacting fermions at high temperature*, Phys. Rev. B **75** (Apr, 2007) 155111.

[16] A. Pal and D. A. Huse, *Many-body localization phase transition*, Phys. Rev. B **82** (Nov, 2010) 174411.

[17] F. Buccheri, A. De Luca, and A. Scardicchio, *Structure of typical states of a disordered richardson model and many-body localization*, Phys. Rev. B **84** (Sep, 2011) 094203.

[18] A. D. Luca and A. Scardicchio, *Ergodicity breaking in a model showing many-body localization*, EPL (Europhysics Letters) **101** (2013), no. 3 37003.

[19] P. Anderson, *Theory of dirty superconductors*, Journal of Physics and Chemistry of Solids **11** (1959), no. 12 26 – 30.

[20] S. Maekawa and H. Fukuyama, *Localization effects in two-dimensional superconductors*, Journal of the Physical Society of Japan **51** (1982), no. 5 1380–1385, [http://dx.doi.org/10.1143/JPSJ.51.1380].

[21] A. Kapitulnik and G. Kotliar, *Anderson localization and the theory of dirty superconductors*, Phys. Rev. Lett. **54** (Feb, 1985) 473–476.

[22] G. Kotliar and A. Kapitulnik, *Anderson localization and the theory of dirty superconductors. ii*, Phys. Rev. B **33** (Mar, 1986) 3146–3157.

[23] M. Ma and P. A. Lee, *Localized superconductors*, Phys. Rev. B **32** (Nov, 1985) 5658–5667.

[24] D. Arean, A. Farahi, L. A. Pando Zayas, I. Salazar Landea, and A. Scardicchio, *A Dirty Holographic Superconductor*, Phys.Rev. **D89** (2014) 106003, [arXiv:1308.1920].

[25] S. A. Hartnoll, P. K. Kovtun, M. Muller, and S. Sachdev, *Theory of the Nernst effect near quantum phase transitions in condensed matter, and in dyonic black holes*, Phys.Rev. **B76** (2007) 144502, [arXiv:0706.3215].

[26] S. A. Hartnoll and C. P. Herzog, *Impure AdS/CFT correspondence*, Phys.Rev. **D77** (2008) 106009, [arXiv:0801.1693].

[27] M. Fujita, Y. Hikida, S. Ryu, and T. Takayanagi, *Disordered Systems and the Replica Method in AdS/CFT*, *JHEP* **0812** (2008) 065, [arXiv:0810.5394].

[28] S. Ryu, T. Takayanagi, and T. Ugajin, *Holographic Conductivity in Disordered Systems*, *JHEP* **1104** (2011) 115, [arXiv:1103.6068].

[29] A. Adams and S. Yaida, *Disordered Holographic Systems I: Functional Renormalization*, arXiv:1102.2892.

[30] A. Adams and S. Yaida, *Disordered Holographic Systems II: Marginal Relevance of Imperfection*, arXiv:1201.6366.

[31] O. Saremi, *Disorder in Gauge/Gravity Duality, Pole Spectrum Statistics and Random Matrix Theory*, *Class.Quant.Grav.* **31** (2014) 095014, [arXiv:1206.1856].

[32] H. B. Zeng, *Possible Anderson localization in a holographic superconductor*, *Phys.Rev.* **D88** (2013) 126004, [arXiv:1310.5753].

[33] S. A. Hartnoll and J. E. Santos, *Disordered horizons: Holography of randomly disordered fixed points*, *Phys.Rev.Lett.* **112** (2014) 231601, [arXiv:1402.0872].

[34] A. Lucas, S. Sachdev, and K. Schalm, *Scale-invariant hyperscaling-violating holographic theories and the resistivity of strange metals with random-field disorder*, *Phys.Rev.* **D89** (2014) 066018, [arXiv:1401.7993].

[35] S. A. Hartnoll and D. M. Hofman, *Locally Critical Resistivities from Umklapp Scattering*, *Phys.Rev.Lett.* **108** (2012) 241601, [arXiv:1201.3917].

[36] J. Sonner, *On universality of charge transport in AdS/CFT*, *JHEP* **1307** (2013) 145, [arXiv:1304.7774].

[37] C. P. Herzog, K.-W. Huang, and R. Vaz, *Linear Resistivity from Non-Abelian Black Holes*, arXiv:1405.3714.

[38] D. Vegh, *Holography without translational symmetry*, arXiv:1301.0537.

[39] M. Blake, D. Tong, and D. Vegh, *Holographic Lattices Give the Graviton a Mass*, *Phys.Rev.Lett.* **112** (2014) 071602, [arXiv:1310.3832].

[40] A. Amoretti, A. Braggio, N. Maggiore, N. Magnoli, and D. Musso, *Thermo-electric transport in gauge/gravity models with momentum dissipation*, arXiv:1406.4134.

[41] A. Amoretti, A. Braggio, N. Maggiore, N. Magnoli, and D. Musso, *Analytic DC thermo-electric conductivities in holography with massive gravitons*, `arXiv:1407.0306`.

[42] I. Amado, D. Arean, A. Jimenez-Alba, K. Landsteiner, L. Melgar, *et. al.*, *Holographic Type II Goldstone bosons*, *JHEP* **1307** (2013) 108, [`arXiv:1302.5641`].

[43] I. Amado, D. Arean, A. Jimnez-Alba, K. Landsteiner, L. Melgar, *et. al.*, *Holographic Superfluids and the Landau Criterion*, *JHEP* **1402** (2014) 063, [`arXiv:1307.8100`].

[44] I. Amado, D. Arean, A. Jimenez-Alba, L. Melgar, and I. Salazar Landea, *Holographic s+p Superconductors*, *Phys.Rev.* **D89** (2014) 026009, [`arXiv:1309.5086`].

[45] P. Basu, J. He, A. Mukherjee, and H.-H. Shieh, *Hard-gapped Holographic Superconductors*, *Phys.Lett.* **B689** (2010) 45–50, [`arXiv:0911.4999`].

[46] M. Ammon, J. Erdmenger, V. Grass, P. Kerner, and A. O'Bannon, *On Holographic p-wave Superfluids with Back-reaction*, *Phys.Lett.* **B686** (2010) 192–198, [`arXiv:0912.3515`].

[47] S. Gangopadhyay and D. Roychowdhury, *Analytic study of properties of holographic p-wave superconductors*, *JHEP* **1208** (2012) 104, [`arXiv:1207.5605`].

[48] D. Roychowdhury, *Holographic droplets in p-wave insulator/superconductor transition*, *JHEP* **1305** (2013) 162, [`arXiv:1304.6171`].

[49] R. E. Arias and I. S. Landea, *Backreacting p-wave Superconductors*, *JHEP* **1301** (2013) 157, [`arXiv:1210.6823`].

[50] B. I. Halperin, *Dynamic properties of the multicomponent bose fluid*, *Phys. Rev. B* **11** (Jan, 1975) 178–190.

[51] P. Phillips, *Advanced solid state physics*. Cambridge University Press, Cambridge New York, 2012.

[52] E. Orlandini, M. C. Tesi, and S. G. Whittington, *Self-averaging in the statistical mechanics of some lattice models*, *Journal of Physics A: Mathematical and General* **35** (2002), no. 19 4219.

[53] K. Binder and A. Young, *Spin glasses: Experimental facts, theoretical concepts, and open questions*, *Rev.Mod.Phys.* **58** (1986) 801–976.

[54] P. Basu, A. Mukherjee, and H.-H. Shieh, *Supercurrent: Vector Hair for an AdS Black Hole*, Phys.Rev. **D79** (2009) 045010, [`arXiv:0809.4494`].

[55] J. Erdmenger, X.-H. Ge, and D.-W. Pang, *Striped phases in the holographic insulator/superconductor transition*, JHEP **1311** (2013) 027, [`arXiv:1307.4609`].

[56] D. Arean et al, *In preparation*, .

[57] L. Dang, M. Boninsegni, and L. Pollet, *Disorder-induced superfluidity*, Phys. Rev. B **79** (Jun, 2009) 214529.

[58] A. Niederberger, J. Wehr, M. Lewenstein, and K. Sacha, *Disorder-induced phase control in superfluid fermi-bose mixtures*, EPL (Europhysics Letters) **86** (2009), no. 2 26004.

[59] L. A. Pando Zayas and D. Reichmann, *A Holographic Chiral $p_x + ip_y$ Superconductor*, Phys.Rev. **D85** (2012) 106012, [`arXiv:1108.4022`].